Towards understanding secondary structure transitions: phosphorylation and metal coordination in model peptides†

Malgorzata Broncel, Sara C. Wagner, Kerstin Paul, Christian P. R. Hackenberger* and Beate Koksch*

Received 22nd January 2010, Accepted 17th March 2010
First published as an Advance Article on the web 29th March 2010
DOI: 10.1039/c001458c

Secondary structure transitions are important modulators of signal transduction and protein aggregation. Phosphorylation is a well known post-translational modification capable of dramatic alteration of protein secondary structure. Additionally, phosphorylated residues can induce structural changes through metal binding. Data derived from the Protein Data Bank demonstrate that magnesium and manganese are metal ions most favored by phosphate. Due to the complexity of molecular interactions as well as the challenging physicochemical properties of natural systems, simplified peptide models have emerged as a useful tool for investigating the molecular switching phenomenon. In this study using a coiled coil model peptide, we show structural consequences of phosphorylation and subsequent magnesium and manganese ions coordination. In the course of our experiment we obtained a switch cascade starting from a stable helical conformation of the control peptide, continuing through the phosphorylation-induced unfolded structure, and ending with a metal-stabilized α-helix (Mg^{2+}) or helical fibers (Mn^{2+}), each of which could be transferred back to the unfolded form upon EDTA chelation. This study demonstrates how small peptide models can aid in the evaluation and a better understanding of protein secondary structure transitions.

Introduction

Switching the secondary structure of peptides and proteins by covalent and non-covalent interactions provides a means to better understand enzyme regulation, gene transcription, and protein aggregation. Investigation of molecular switching in response to site-specific modifications, *e.g.* phosphorylation, often requires chemical access to a particular system. In the case of a peptide, site-specific modifications can be introduced by a robust building block solid phase peptide synthesis (SPPS) strategy. Despite the availability of chemical tools that give access to specifically modified proteins,[1] detailed structural studies of such large molecules can sometimes be hampered by the complex and challenging physicochemical properties of the system. In order to overcome these obstacles, the development and application of simplified peptide model systems for studying the molecular switching phenomenon is of great interest.[2] The advantage of models is that they are intrinsically simple in comparison to their natural counterparts, yet still possess sufficient complexity in structure for studying protein folding and function.

One of the most explored model systems is based on the coiled coil structural folding motif. Coiled coils are biologically relevant, simple, yet versatile.[3,4] They consist of at least two α-helices wrapped around each other in a slight superhelical twist. The primary structure is characterized by a periodicity of seven residues, the so-called *heptad*, which is commonly denoted $(a\text{-}b\text{-}c\text{-}d\text{-}e\text{-}f\text{-}g)_n$ (Fig. 1). Positions *a* and *d* are typically occupied by nonpolar residues that form the first recognition domain by hydrophobic core packing ("knobs-into-holes"). Charged amino acids at positions *e* and *g* form the second recognition motif and engage in interhelical electrostatic interactions. Polar residues are often found at the remaining heptad repeat positions *b*, *c*, and *f*, which are solvent exposed.

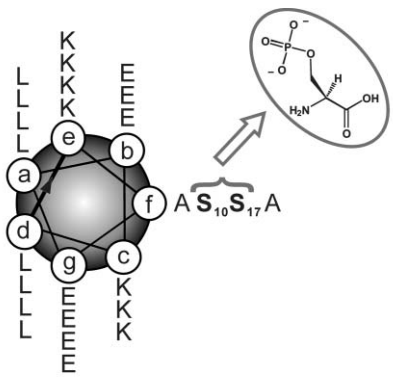

Fig. 1 Helical wheel representation of the control peptide (CP) and sequences of synthesized model peptides.

The application of coiled coil-based models as tools for understanding structural transitions in response to such stimuli like pH, metal ions, unnatural amino acids, and post-translational modifications has been described.[5–11] In most cases, however, the impact of only one factor was probed at a time.

In this report we aim to study the sequential impact of two closely connected stimuli, phosphorylation and metal ions, on the secondary structure of peptides. We have directed our attention

Institut für Chemie und Biochemie, Freie Universität Berlin, Takustr. 3, 14195 Berlin, Germany. E-mail: koksch@chemie.fu-berlin.de, hackenbe@chemie.fu-berlin.de; Fax: +49-30-838-55644; Fax: +49-30-838-52551; Tel: +49-30-838-55344; Tel: +49-30-838-52451

† Electronic supplementary information (ESI) available: Additional HPLC, SEC and CD data. See DOI: 10.1039/c001458c

towards these factors as they have profound impact on protein folding and function, both in cellular processes and human disease. For instance, in eukaryotic cells phosphorylation-induced conformational changes are the basis for signal transduction,[12] whereas metal ions play crucial roles in protein stabilization, electron transfer, and enzymatic catalysis.[13] On the other hand, accumulated evidence points to a role of both phosphorylation and metals in protein misfolding and aberrant aggregation.[14,15] Elucidating the effect of these two stimuli on the secondary structure in model systems is therefore of great interest. It may allow better understanding of molecular switching, and furthermore shed some light on more complex protein-protein interactions.

Previously, the impact of phosphorylation on the helical structure was a subject of extensive study. In general, phosphorylation of helices is destabilizing either due to electrostatics (especially at the C-terminus) or to the high desolvation penalty associated with the bulky side chain (mainly in the helix interior).[16,17] Stabilizing interactions involving phosphate moieties are possible only at positively charged N-terminus of the helix[10,16] or by the involvement of the phosphate into attractive Coulombic interactions with neighboring residues.[18,19]

Herein we use phosphorylation as a starting point for subsequent metal coordination studies. We explored a coiled coil model, which was *de novo* designed to possess a stable, well defined helical fold. The key design features of our control peptide (CP) are as follows (Fig. 1): hydrophobic leucine residues at positions *a* and *d* in combination with interhelical electrostatic attractions between glutamate and lysine at positions *e* and *g* ensure stability of the α-helical coiled coil structure; an introduction of glutamate (position *b*) and lysine (position *c*) provides further helix stabilization due to the attractive electrostatic interactions in the intrahelical fashion between *b* - *e* and *c* - *g* positions, respectively; position *f* of the CP, which is not part of any of the main recognition domains, has been used to incorporate two phosphoserine residues to yield peptide P (10,17).

Results and discussion

Phosphorylation impact on the secondary structure

In agreement with our design strategy, circular dichroism (CD) spectra of 100 μM CP at pH 7.4 showed α-helical folding characterized by the appearance of two minima at 208 and 222 nm (Fig. 2). The intensity of CD signal at 222 nm suggested a helical content of approximately 70%. Size exclusion chromatography (SEC) was used to characterize the oligomerization state of CP and revealed the presence of trimeric species (see ESI†). The stability of the helical folding was examined by thermal denaturation. We have found that at 100 μM concentration, CP can not be completely unfolded by heat, even upon addition of 3.5 M urea (data not shown). Therefore thermal denaturation of 40 μM peptide in the presence of 3 M urea was performed and gave a melting temperature (T_M) of 67 °C (Supporting Information), which is consistent with a good thermal stability of the helical fold.

A significant change in CP structure was imposed by the introduction of a phosphate moiety. The CD signature of 100 μM P (10,17) at pH 7.4 indicated the presence of mainly unfolded species with a predominant minimum at 204 nm (Fig. 2). Significant

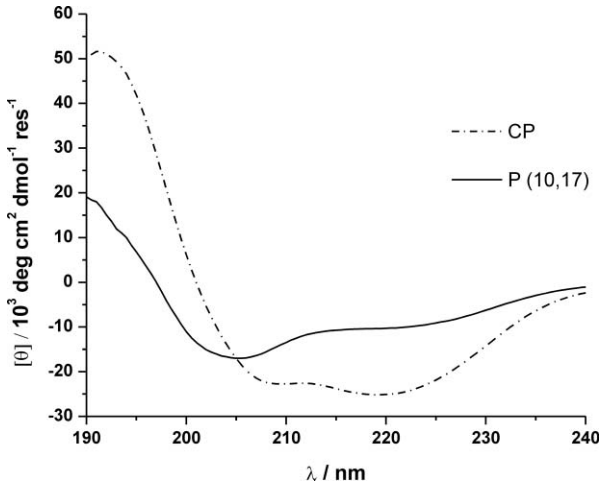

Fig. 2 CD spectra of 100 μM peptides in 10 mM Tris/HCl buffer, pH 7.4.

increase in ellipticity at 222 nm reflected in almost 40% decrease in the helical content. Furthermore, thermal melting of 40 μM P (10,17) in the presence of 3 M urea showed that phosphorylation results in the reduction of T_M to 41 °C (see ESI†). All these facts point to a significant destabilization of the helical structure upon introduction of the phosphate moiety. Surprisingly, SEC of P (10,17) did not indicate any significant changes in the oligomerization state with respect to CP (see ESI†). The only difference is the presence of a small fraction of dimeric species. One justification for this behavior may be the fact that despite the predominantly unfolded nature of P (10,17), the 30% reminiscence of helical structure is apparently sufficient to prevent complete dissociation of individual helices from the initial coiled coil trimer.

Structural effects of phosphate can be attributed to the charged and bulky nature of this group (see above). In our system the electrostatics are likely to be a driving force for the unfolding of P (10,17). Specifically, intramolecular Coulombic repulsions between positions *b* and *f* occupied by glutamate and phosphate, respectively, could destabilize the helix monomer. This destabilization is obviously in a strong competition to the cooperative interactions that promote coiled coil formation. Since electrostatic repulsions between amino acid side chains in coiled coils can be diminished by the presence of charged co-solutes,[6] we performed a salt screening experiment with the use of 0.2 M NaCl to test our hypothesis (see ESI†). Our results indicate that charge neutralization yields a significant (almost 30%) increase in helicity of P (10,17) and further confirm that the source of phosphate-induced conformational change is of ionic origin.

Metal coordination to P (10,17)

Taking into account that phosphorylated residues can also induce structural transitions *via* metal binding,[20–22] we used P (10,17) as a starting point for metal coordination studies. Specifically, we wanted to take advantage of the phosphate coordinating properties seen in proteins. Data derived from the Protein Data Bank show that magnesium and manganese are the metals most favored by phosphate.[23] Reports addressing the use of various metal ions for the induction of conformational transitions within coiled coils have been published (for a review see ref. 13). In most cases, however, Cys, His, and specific residues, such as

2,2′-bipyridine or iminodiacetic acid have been introduced to a peptide sequence to allow for a specific binding of a metal ion. To our knowledge the phosphate group, especially in combination with either Mg^{2+} or Mn^{2+}, has not been used to serve this purpose so far. Given the fact that: 1) Mg^{2+} is the most ubiquitous divalent cation in cells while Mn^{2+} is the most common surrogate of Mg^{2+},[24] 2) both ions have been found coordinated to phosphates,[23] and finally 3) phosphorylated proteins constitute for about 30% of the proteome,[25] we were very much encouraged to probe the behavior of P (10,17) in the presence of varying concentrations of Mg^{2+} and Mn^{2+} ions.

Upon addition of either metal, 100 μM P (10,17) at pH 7.4 undergoes a vigorous transition from predominantly random coil towards helical structure (Fig. 3). Titration of phosphorylated peptide with Mg^{2+} (Fig. 3a), produces CD signatures with well developed minima at 208 and 222 nm, which together with the appearance of the isodichroic point at 204 nm, is consistent with a quasi-two-state random coil-helix conformational transition. Additionally, SEC of P (10,17) containing 2 mM $MgCl_2$ confirmed the presence of a trimeric coiled coil containing a small fraction of dimeric species (see ESI†). Similarly, Mn^{2+} titration gives origin to the helical structure as monitored by CD spectroscopy (Fig. 3b). In the case of Mn^{2+}, however, structural transition appears to be more

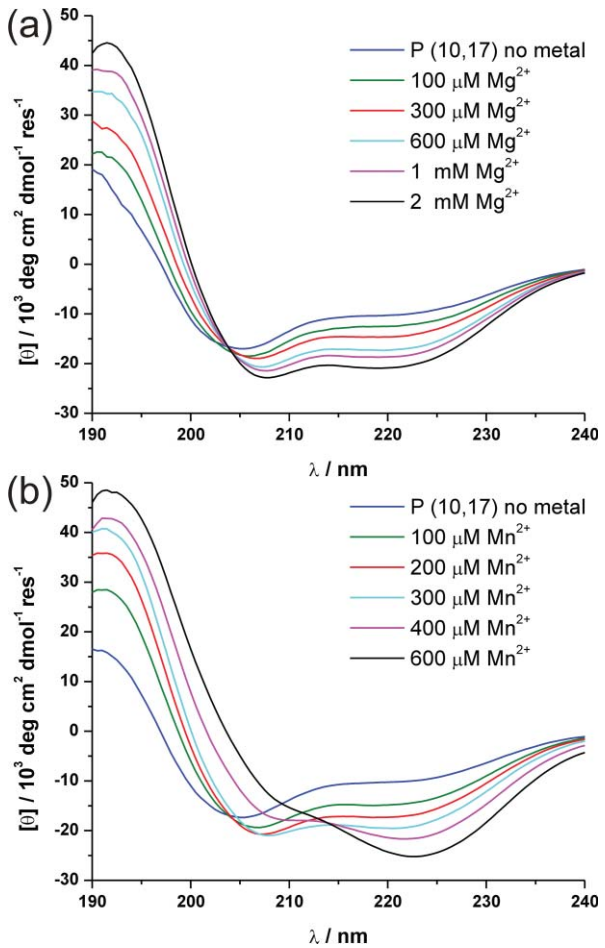

Fig. 3 Titration of 100 μM P (10,17) in 10 mM Tris/HCl buffer, pH 7.4 with different concentrations of $MgCl_2$ (a) and $MnCl_2$ (b) monitored by CD spectroscopy.

complex. First of all, the isodichroic point is lost, and moreover, observed helical signatures possess an increased $[\theta]_{222}/[\theta]_{208}$ peak ratio, which suggests the presence of helical aggregates.[26] Indeed, transmission electron microscopy (TEM) of Mn^{2+} treated P (10,17) confirmed the existence of long, rigid and non-branched fibers consisting of ~2 nm wide protofilaments (Fig. 4). The measured protofilament width would allow an arrangement of 3-4 α-helices along the protofilament axis.[27] The presence of aggregates becomes evident already during the titration experiment, since starting from 400 μM concentration of manganese a white precipitate appears. In contrast, Mg^{2+} titrated peptide is fully soluble up to a metal concentration of 2 mM.

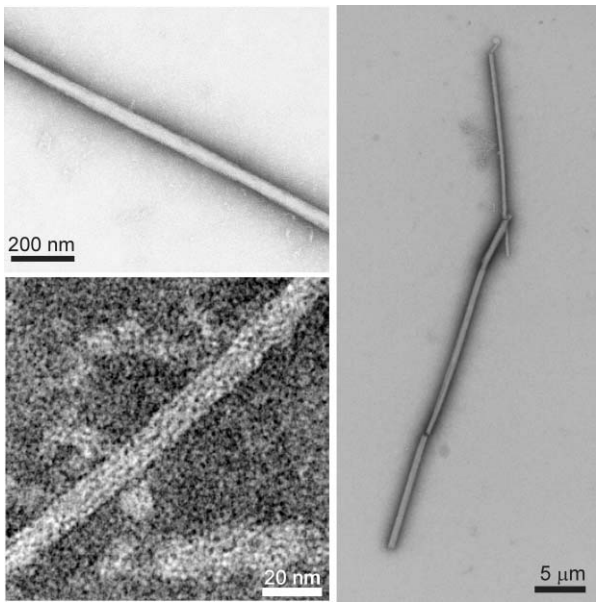

Fig. 4 TEM micrographs of fibers of 100 μM P (10,17) incubated with 300 μM $MnCl_2$ in 10 mM Tris/HCl buffer, pH 7.4.

A detailed examination of Fig. 3 suggests that Mn^{2+} is a more efficient structure inducer than Mg^{2+}. For comparison, the helical content of P (10,17) in the presence of 300 μM Mn^{2+} or Mg^{2+} equals 54% or 40%, respectively. Furthermore, the stoichiometry of metal binding evaluated by atomic absorption spectroscopy (AAS) under the above-mentioned conditions indicates that Mn^{2+} is coordinated more efficiently than Mg^{2+}. The experiment showed that the peptide binds Mn^{2+} in an almost 1 : 1 ratio (1 : 0.9 ± 0.1 (2)), whereas the content of Mg^{2+} is over two fold smaller (1 : 0.40 ± 0.03 (2)). This difference can be explained by the higher affinity of Mn^{2+} ions towards the phosphate group.[28,29] Moreover, the fact that our negative control (unphosphorylated CP) showed binding of both metals in the ratio of approximately 1 : 0.1 suggests that even though other residues, most probably glutamic acids, also contribute to the overall metal content of P (10,17), the structural transitions we observe are predominantly due to metal coordination to the phosphate group. This result is in agreement with the CD monitored metal titration of the CP (see ESI†), which showed no structural transitions even at the highest metal concentrations tested (600 μM and 2 mM for Mn^{2+} and Mg^{2+}, respectively).

Despite the apparent difference between both metals in the coordination to the phosphate group, the structure-inducing property

is their common denominator. In order to unambiguously prove the involvement of metal ions in this process, the specificity of metal effect was investigated by the removal of Mn^{2+} and Mg^{2+} with the use of EDTA (Fig. 5). Again, for better comparison metal concentration was fixed at 300 μM, whereas peptide concentration was kept constant at 100 μM. Addition of 1 eq. of EDTA to manganese-peptide complexes results in the loss of helical structure and restoration of the initial, predominantly unfolded species (Fig. 5a). Helical structure induced by Mg^{2+} also switches back, however, metal scavenging by EDTA is not as efficient as in the case of Mn^{2+} (Fig. 5b). This fact can be attributed to the lower binding constant of Mg^{2+} to EDTA.[24] Our experiment shows that the new helical structures are metal-dependent and that the effect of metal ions on the secondary structure is reversible.

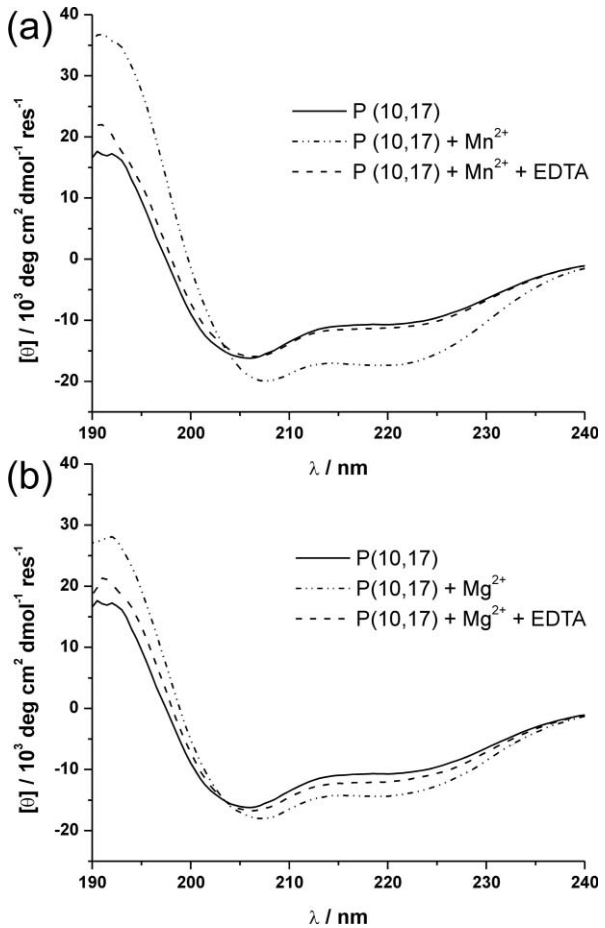

Fig. 5 CD spectra of 100 μM P (10,17) in 10 mM Tris/HCl buffer, pH 7.4 incubated with 300 μM $MnCl_2$ (a) and 300 μM $MgCl_2$ (b) in the presence of 300 μM EDTA.

Conclusions

In summary, using a simple yet versatile coiled coil-based model we were able to probe the influence of two biologically relevant factors, phosphorylation and metal ions, on the helical structure. Importantly, we focused on the sequential impact of both stimuli, and took advantage of the fact that phosphorylated residues can induce structural transitions *via* metal binding. To our knowledge, no previous reports describing structural consequences of the coordination of magnesium and manganese to phosphoproteins are available, which is quite surprising, as both metals are favored by phosphate. Our results point to a significant molecular switching ability of both tested stimuli, with phosphorylation being highly destabilizing and metals possessing structure-inducing properties. In the course of our experiment we obtained a switch cascade starting from a stable helical conformation of the CP, continuing through the unfolded P (10,17), and ending with a metal-stabilized α-helix (Mg^{2+}) or helical fibers (Mn^{2+}), each of which could be transferred back to the unfolded form by EDTA chelation. The study described herein is a great example for small peptide models being versatile tools to study a dynamic nature of the secondary structure in response to various stimuli. Owing to the intrinsic simplicity of the model, the principles of protein folding can be studied in detail and further carried over to more complex systems, thus providing a great help in the understanding of protein structure and function.

Experimental

Peptide synthesis

Peptides were synthesized on a SyroXP-I peptide synthesizer (Multi-SynTech GmbH) according to standard Fmoc/tBu chemistry using TBTU/HOBt and preloaded Fmoc-Leu-Wang resin (Novabiochem). Fmoc-Ser(PO(OBzl)OH)-OH (Bachem) was activated with HATU/DIEA and coupled manually to the resin. DIEA was added in 3-fold excess with respect to the amino acid and HATU. The reaction time was extended to 6 h. Peptides were N-terminally labelled with anthranilic acid (Abz). A mixture of DBU and piperidine (2% each) in DMF was used for Fmoc deprotection. Peptides were cleaved from the resin by treatment with 2 mL TFA/TIS/H_2O (95/2.5/2.5) for 3 h following by precipitation with cool diethyl ether. Purification was carried out by preparative reversed phase HPLC on a Knauer Smartline system (Knauer GmbH) equipped with a Luna™ C8 (10 μm, 250 × 21.20 mm) column (Phenomenex) running with water/0.1% TFA and ACN/0.1% TFA gradient at 20 mL min^{-1}. Purified peptides were characterized by analytical HPLC (see ESI†) and HRMS (ESI-TOF): CP *m/z*: 1053.6164 $[M+3H]^{3+}$ (calcd.: *m/z*: 1053.6149); P (10,17) *m/z*: 1106.9237 $[M+3H]^{3+}$ (calcd.: *m/z*: 1106.9257).

Sample preparation

Peptides were dissolved in 10 mM Tris/HCl buffer, pH 7.4 immediately before measurements. Peptide concentrations were estimated by $UV_{320\,nm}$ absorption characteristic for Abz (calibration curve was recorded) and adjusted to 100 μM. Titrations with aqueous $MgCl_2$ and $MnCl_2$ (50 mM) were performed in a range of concentrations: 100–600 μM (Mn^{2+}) and 0.1–2 mM (Mg^{2+}). When appropriate, chelation of metal ions (300 μM) was accomplished by addition of EDTA (300 μM).

Samples for AAS (100 μM peptides, 300 μM metal ions, 10 mM Tris/HCl buffer, pH 7.4) were incubated overnight and centrifuged in Amicon Ultra–0.5 mL 3 K centrifugal filters (Millipore) at 14 000 g in order to remove all unbound metal. Peptides were washed twice with deionized water and diluted to 100 μM. Peptide content was confirmed by UV measurement.

Circular dichroism

CD spectra were recorded on a Jasco J-810 spectropolarimeter at 20 °C (Jasco GmbH) using 0.1 cm Quartz Suprasil® cuvettes (Hellma). Spectra were averaged over three scans (240–190 nm, 0.5 nm intervals, 1 nm bandwidth, 1 s response time) and background corrected. Ellipticity was normalized to concentration (c/mol L^{-1}), number of residues ($n = 27$, including the N-terminal label Abz) and path length (l/cm) using eqn (1), where θ_{obs} is the measured ellipticity in mdeg and [θ] the mean residue ellipticity in 10^3 deg cm^2 dmol^{-1} residue^{-1}.

$$[\theta] = \theta_{obs}/(10000 \cdot l \cdot c \cdot n) \quad (1)$$

Transmission electron microscopy

Sample of peptide P (10,17) containing 300 μM $MnCl_2$ from CD-measurement was incubated overnight and 6 μL aliquots of the solution were placed for 60 s on glow-discharged (60 s plasma treatment at 8 W in a BALTEC MED 020) carbon-coated collodium support films covering 400-mesh copper grids (BALTEC, Lichtenstein). After blotting and negative staining with phosphotungstic acid (PTA, 1%), the grids were left to air-dry. TEM images were recorded with a Philips CM12 transmission electron microscope (FEI company, Oregon, USA) at 100 kV accelerating voltage and at primary magnification 58000x on Kodak SO-163 negative film by using a defocus of 0.9 nm. Image J (version 1.38x, Wayne Rasband, USA) was used for the determination of the diameter of peptide fibers.

Calculation of α-helicity

The helical content of all peptides was calculated using the characteristic CD mean residue ellipticity [θ] at 222 nm in deg cm^2 dmol^{-1}. The respective value for 100% helicity in a 27 residue peptide was calculated using the equation:

$$[\theta]^n_H = -39500 \cdot (1 - 2.57/n) \quad (2)$$

where $[\theta]^n_H$ and −39500 are the mean residue ellipticities of a helix of n and infinite residues at 222 nm in deg cm^2 dmol^{-1}, 2.57 is a chain-length-dependent factor at 222 nm, and n is the number of residues.[30]

Atomic absorption spectroscopy

Samples containing Mn^{2+} were prepared as described above and analyzed on ZEEnit 600 graphite furnace atomic absorption spectrometer (AnalytikJena). Mn^{2+} was detected with a hollow cathode lamp at 279.5 nm with a bandpass of 0.2 nm. Zeeman method was used for background correction. Samples were diluted with double distilled water and injected (20 μL) into graphite wall tubes. Pyrolysis and atomization temperatures were set to 1000 °C and 1600 °C, respectively. The mean AUC (area under curve) absorptions of duplicate injections were used throughout the study.

Samples containing Mg^{2+} were prepared as described above and analyzed on a Vario 6 flame atomic absorption spectrometer (AnalytikJena). Mn^{2+} was detected with a hollow cathode lamp at 285.2 nm with a bandpass of 1.2 nm. A deuterium lamp was used for background correction. Samples were diluted with double distilled water and injected (~ 3 mL) into the flame (C_2H_2/air, delivered at 50 L h^{-1}). Burner height was 8 mm and aspiration rate was set to 5 mL min^{-1}. The mean AUC (area under curve) absorptions of five injections were used throughout the study.

The metal content of the samples was assessed by the linear extrapolation method.

Acknowledgements

We are grateful to Heike Scheffler and Magnus Krüger from Prof. Ronald Gust's laboratory (Institüt fur Pharmazie, Freie Universität Berlin) for their help with the AAS measurements. We also thank Dr P. Winchester for proofreading this manuscript. This work was supported by the Deutsche Forschungsgemeinschaft (SFB 765 - Multivalency as chemical organisation and action principle).

Notes and references

1 C. P. Hackenberger and D. Schwarzer, *Angew. Chem., Int. Ed.*, 2008, **47**, 10030–10074.
2 K. Pagel and B. Koksch, *Curr. Opin. Chem. Biol.*, 2008, **12**, 730–739.
3 D. N. Woolfson, *Adv. Protein Chem.*, 2005, **70**, 79–112.
4 P. Burkhard, J. Stetefeld and S. V. Strelkov, *Trends Cell Biol.*, 2001, **11**, 82–88.
5 K. Pagel, S. C. Wagner, K. Samedov, H. von Berlepsch, C. Böttcher and B. Koksch, *J. Am. Chem. Soc.*, 2006, **128**, 2196–2197.
6 K. Pagel, S. C. Wagner, R. Rezaei Araghi, H. von Berlepsch, C. Böttcher and B. Koksch, *Chem.–Eur. J.*, 2008, **14**, 11442–11451.
7 K. Pagel, T. Seri, H. von Berlepsch, J. Griebel, R. Kirmse, C. Böttcher and B. Koksch, *ChemBioChem*, 2008, **9**, 531–536.
8 K. Pagel, T. Vagt, T. Kohajda and B. Koksch, *Org. Biomol. Chem.*, 2005, **3**, 2500–2502.
9 M. Salwiczek, S. Samsonov, T. Vagt, E. Nyakatura, E. Fleige, J. Numata, H. Colfen, M. T. Pisabarro and B. Koksch, *Chem.–Eur. J.*, 2009, **15**, 7628–7636.
10 R. S. Signarvic and W. F. DeGrado, *J. Mol. Biol.*, 2003, **334**, 1–12.
11 S. Mehta, M. Meldal, V. Ferro, J. Ø. Duus and K. Bock, *J. Chem. Soc., Perkin Trans. 1*, 1997, 1365–1374.
12 T. Hunter, *Cell*, 2000, **100**, 113–127.
13 R. H. Holm, P. Kennepohl and E. I. Solomon, *Chem. Rev.*, 1996, **96**, 2239–2314.
14 A. Alonso, T. Zaidi, M. Novak, I. Grundke-Iqbal and K. Iqbal, *Proc. Natl. Acad. Sci. U. S. A.*, 2001, **98**, 6923–6928.
15 A. I. Bush, *Curr. Opin. Chem. Biol.*, 2000, **4**, 184–191.
16 C. D. Andrew, J. Warwicker, G. R. Jones and A. J. Doig, *Biochemistry*, 2002, **41**, 1897–1905.
17 L. Szilak, J. Moitra, D. Krylov and C. Vinson, *Nat. Struct. Biol.*, 1997, **4**, 112–114.
18 N. Errington and A. J. Doig, *Biochemistry*, 2005, **44**, 7553–7558.
19 L. Szilak, J. Moitra and C. Vinson, *Protein Sci.*, 1997, **6**, 1273–1283.
20 L. L. Liu and K. J. Franz, *J. Am. Chem. Soc.*, 2005, **127**, 9662–9663.
21 S. Balakrishnan and N. J. Zondlo, *J. Am. Chem. Soc.*, 2006, **128**, 5590–5591.
22 L. Settimo, S. Donnini, A. H. Juffer, R. W. Woody and O. Marin, *Biopolymers*, 2007, **88**, 373–385.
23 URL: http://tanna.bch.ed.ac.uk/mphos/mphos3w.htm [last accessed January 2010].
24 M. E. Maguire and J. A. Cowan, *BioMetals*, 2002, **15**, 203–210.
25 P. Cohen, *Eur. J. Biochem.*, 2001, **268**, 5001–5010.
26 M. J. Pandya, G. M. Spooner, M. Sunde, J. R. Thorpe, A. Rodger and D. N. Woolfson, *Biochemistry*, 2000, **39**, 8728–8734.
27 P. B. Harbury, P. S. Kim and T. Alber, *Nature*, 1994, **371**, 80–83.
28 D. S. Marynick and H. F. Schaefer, 3rd, *Proc. Natl. Acad. Sci. U. S. A.*, 1975, **72**, 3794–3798.
29 S. S. Massoud and H. Sigel, *Inorg. Chem.*, 1988, **27**, 1447–1453.
30 Y. H. Chen, J. T. Yang and K. H. Chau, *Biochemistry*, 1974, **13**, 3350–3359.